

# Temperature–HF fugacity trends during crystallization of calcite carbonatite magma in the Fen complex, Norway

TOM ANDERSEN AND HÅKON AUSTRHEIM

Mineralogisk–Geologisk Museum, Sars gate N-0562 Oslo 5, Norway

## Abstract

Calcite carbonatite (søvite), associated apatite cumulates and contact metasomatic phlogopite-rocks in the Fen complex (S. Norway) contain coexisting apatite and phlogopite. Two distinct compositional groups are recognized: fluorapatite ( $X_F = 0.5–0.8$ ) coexists with hydroxy-phlogopite with  $X_F = 0.11–0.26$ , whereas hydroxyapatite ( $X_F = 0.34–0.44$ ) coexists with low-F hydroxy-phlogopite ( $X_F \approx 0.03$ ). Apatite–biotite geothermometry suggests that the minerals equilibrated at igneous temperatures (less than 1200 to *ca.* 625 °C), and were not significantly disturbed by late low-temperature re-equilibration. This, combined with HF-barometry based on apatite–fluid and phlogopite–fluid F–OH exchange equilibria, makes it possible to recognize two crystallization trends at different levels of hydrogen fluoride fugacity. The existence of such trends reflects internal buffering of the HF fugacity by apatite and/or phlogopite. The recorded differences in HF fugacity suggest that two or more independent or semi-independent lines of magmatic descent gave rise to calcite carbonatite magma in the Fen complex. Combined apatite–phlogopite geothermometry and hydrogen fluoride barometry is a useful tool enabling us to see through post-magmatic alteration of carbonatites, and to establish primary magmatic controls even in cases where carbonate and iron–titanium oxide minerals have re-equilibrated at much lower temperatures.

KEYWORDS: calcite, carbonatite, søvite, fugacity, Fen complex, Norway.

## Introduction

FLUORINE is a minor element in carbonatites; whole-rock fluorine concentrations are commonly well below one weight percent (e.g. Heinrich, 1966; Dawson and Fuge, 1980; Bailey, 1980). Nevertheless, processes involving fluoride-complexing of metal ions have been assumed to be involved in the generation of carbonatites and the rare-element deposits sometimes associated with them (e.g. Möller *et al.*, 1980; Andersen, 1986b).

Several specific fluorides or fluorine-bearing minerals may be found in carbonatites: fluorite, bastnäsite, parisite, pyrochlore, cryolite (Heinrich, 1966; Clark, 1984; Bailey, 1980; Hogarth, 1989). The most abundant fluorine-bearing minerals in many calcite and dolomite carbonatites are, however, apatite and phlogopite (Heinrich, 1966). These two minerals belong to the common liquidus phases of normal, non-peralkaline calcite carbonatite magma, and also

form in metasomatic processes induced by such carbonatite magmas or by fluids exsolving from them (e.g. Andersen, 1986a, 1989). In carbonatite magmas, crystallization of apatite and phlogopite may buffer the HF activity of the system, and thus influence the distribution of fluorine-complexed trace components.

Traditional geothermometry based on calcite–dolomite and titanomagnetite–ilmenite solvi has restricted applicability in carbonatites, because of low-temperature re-equilibration problems (Gittins, 1979; Andersen, 1984). Since the hydroxyl and fluorine contents of apatite and biotite are functions of both crystallization temperature and hydrogen fluoride fugacity (Munoz and Ludington, 1974; Korshinskij, 1981), these minerals constitute a potential geothermometer (Stormer and Carmichael, 1971) and HF barometer (Munoz, 1984; Yardley, 1985). Some experimental data on F–OH exchange between apatite and fluid suggest that apatite may be less vulnerable to sub-solidus re-equilibration than

carbonates and oxides (Tacker and Stomer, 1989). In spite of this, few results of apatite-biotite geothermometry and HF barometry in carbonatite petrology have been published (Chernysheva *et al.*, 1976; Hogarth *et al.*, 1987; but see also mineralogical papers giving data on the fluorine contents of apatite from carbonatites: Le Bas and Handley, 1979; Sommerauer and Katz-Lehnert, 1985a,b; Knudsen and Rønsbo, 1989).

The present paper reports the result of a case study of fluorine-distribution between apatite and phlogopite in some calcite carbonatites and associated rocks from the Fen complex in S.E. Norway. The purpose of the study has been to explore the potential of combined apatite-phlogopite geothermometry and HF-barometry applied to carbonatites, and to gain insight into the behaviour of fluorine during magmatic and post-magmatic processes in such carbonatites.

### Geological setting

The Fen complex (540 Ma, Andersen and Taylor, 1988) is situated in Telemark in south-east Norway, within Precambrian gneisses (Fig. 1). It was among the first carbonatite and peralkaline silicate rock complexes to be recognized (Brøgger, 1921), which has made it a classical occurrence of its kind. Accounts of its geology, petrology, emplacement- and metasomatic history are given by Sæther (1957), Bergstøl and Svinndal (1960), Barth and Ramberg (1966) and in more recent, specialized studies by Verschure and Maijer (1984), Kresten and Morogan (1986), Andersen (1984, 1986a, 1987, 1988a,b, 1989) and Andersen and Qvale (1986).

One of the most abundant types of carbonatite in the Fen complex is white, granular søvite (calcite carbonatite) with phlogopite, apatite, alkali-calcic amphibole, magnetite and pyrite as minor constituents. This rock forms veins, dykes and larger, dyke-like intrusive bodies in the central part of the Fen complex (Sæther, 1957; Andersen, 1986a, 1989). The søvite is associated with younger and less abundant dykes of yellowish granular dolomite carbonatite, containing apatite and minor amphibole, but little or no phlogopite. Some of the søvite and dolomite carbonatite intrusions contain centimetre- to metre-sized inclusions, ranging in composition from apatite-rock with minor phlogopite to apatite-phlogopite carbonatite. In the carbonate-rich inclusions, apatite and phlogopite occur as subhedral phenocrysts in a granular carbonate matrix, similar to what is seen in carbonatite dykes sampled at the surface. In the carbonate-

poorer inclusions, euhedral to subhedral zoned biotite crystals are set in a matrix of prismatic apatite, in part as inclusions in single apatite crystals. The textures of these rocks are different from contact metasomatic apatite-phlogopite rocks (Andersen, 1989), and they are interpreted as products of igneous crystallization. Primary mineral and fluid inclusions in apatite suggest that the apatite-rich rocks have formed by accumulation of apatite  $\pm$  phlogopite from carbonatite magma at some depth in the crust ( $P \geq 4$  kbar); pieces of this cumulate were brought to the present surface as cognate xenoliths in carbonatite magma (Andersen, 1986a). Observation of possible mafic silicate glass inclusions in apatite crystals from the mid-crustal cognate cumulate xenoliths (Andersen, 1986a), and textural evidence of immiscible coexistence of calcite carbonatite and mafic silicate melts in certain types of the damtjernite intrusions in the Fen complex (Griffin and Taylor, 1975; Dahlgren, 1984, 1987) suggest that the carbonatite magma may have originated from a mafic silicate precursor by a liquid immiscibility process taking place in the middle crust (Andersen, 1986a).

The country-rock of the søvite and dolomite carbonatite intrusions is a fenite, i.e. an alkali metasomatized gneiss, composed of alkali feldspar(s), aegirine-augite and alkali amphibole (Brøgger, 1921; Kresten and Morogan, 1986). The fenite formed by metasomatic transformation of Precambrian granitic gneisses by fluids emanating from peralkaline magmas (ijolite, peralkaline calcite carbonatite) emplaced before the rocks of the søvite-dolomite carbonatite association intruded (Sæther, 1957; Kresten and Morogan, 1986; Verschure and Maijer, 1984; Andersen, 1989). Along the intrusive contacts, søvite and dolomite carbonatite are lined by zones of phlogopite + alkali amphibole + calcite + apatite. These zones range in width from millimetres when found along veinlets, to tens of metres when associated with major intrusive bodies of dyke-swarms. These zones formed by magnesium contact metasomatism of feldspathic fenite, induced by the carbonatite magma (Andersen, 1989).

From a study of carbonatite mineralogy and stable and radiogenic isotope data, Andersen (1984) demonstrated that hematite carbonatites in the eastern part of the Fen complex re-equilibrated with groundwater at  $T < 300^\circ\text{C}$ . Density and compositional characteristics of fluid inclusions in matrix calcite of søvites suggest that the rocks of this study were also disturbed at similar, low sub-solidus temperatures, but that they interacted with fluids of magmatic origin

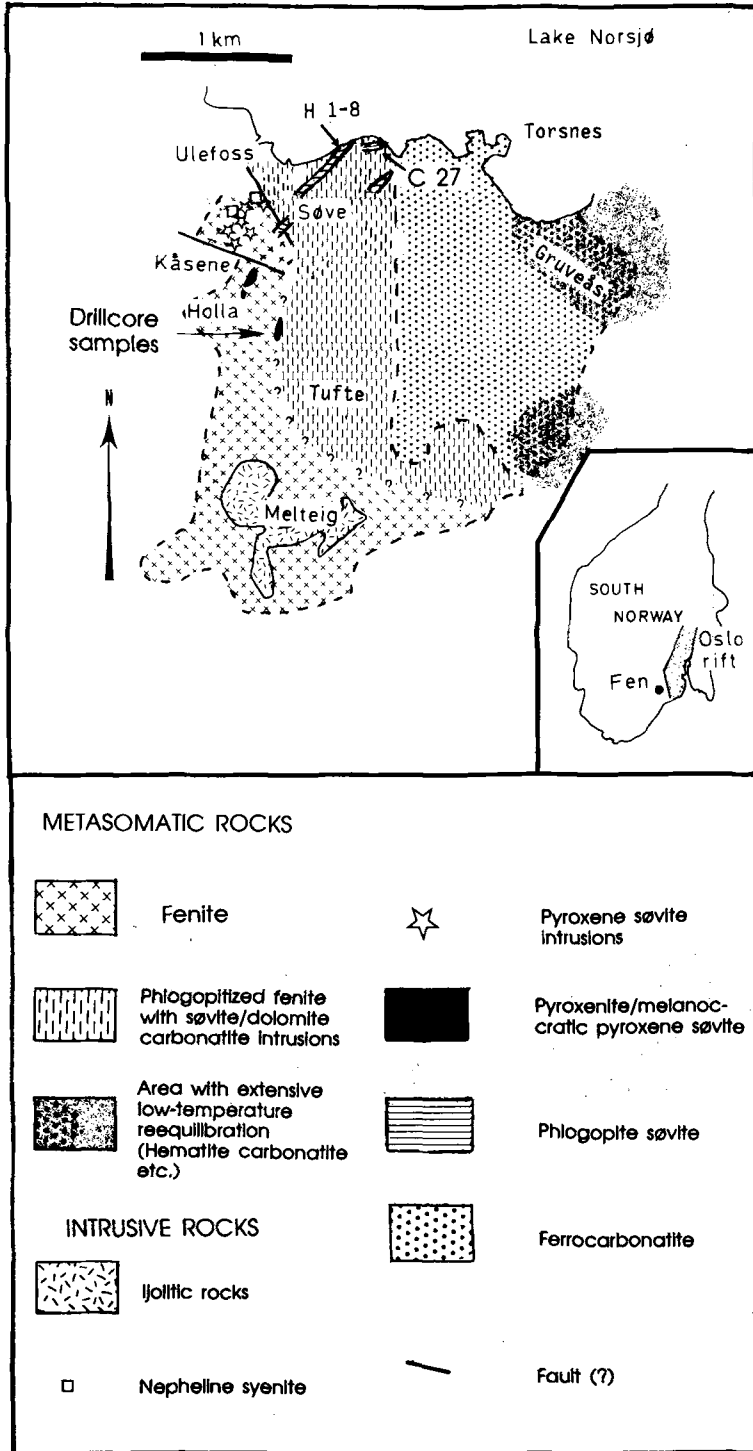


Fig. 1. Simplified geological map of the Fen carbonatite complex, with sample localities indicated.

(Andersen, 1988b). During re-equilibration of carbonatites, both the distribution of Ca and Mg between coexisting calcite and dolomite and the Fe-Ti oxide mineralogy of the carbonatites have been disturbed; the most important silicate mineral reaction is the breakdown of phlogopite to chlorite (Andersen, 1984).

### Petrography

The samples studied have been chosen from a larger collection to cover the petrographic spectrum of phlogopite-apatite bearing rocks. The samples were taken from fresh surface exposures (letter + number) as well as from drillcores (composite numbers: drill-core no./depth in metres along core). Sample 1/9.60 is a partly recrystallized apatite cumulate with phlogopite and abundant pyrochlore inclusions in apatite. Samples 1/21.70 and 4/64.50 are apatite-rich calcite carbonatites with minor phlogopite, 4/64.50 also contains pyrochlore. In 1/21.70 phlogopite forms millimetre-sized laths intergrown with prismatic apatite; the phlogopite contains apatite inclusions. Towards apatite, the phlogopite changes from 'normal' pleochroism (x: pale yellow, y,z: pale green) to 'inverse' (x: orange brown, y,z: pale green). Sample 3/84.80 is a calcite-dolomite carbonatite without fresh biotite, containing minor amounts of brown, subhedral baddeleyite.

Samples H 8 and C 27 come from søvite dykes sampled at the surface; they contain phlogopite and amphibole as phenocryst phases, and partly resorbed dolomite. Both samples have phlogopite with inverse pleochroism. H 1 and H 1-2 are two thin-sections of a large hand-specimen of søvite-veined contact metasomatic phlogopite-amphibole rock. The søvite vein (H 1-2) contains subhedral apatite and phlogopite macrocrysts in a granular calcite matrix. Apatite also occurs as a lining along the intrusive contacts, and dispersed within the phlogopite-amphibole rock (H 1). All phlogopite in this rock has normal pleochroism.

### Composition of apatite and phlogopite

#### Analytical methods

Apatite and phlogopite were analysed for major elements on a fully automatic Cameca CAMEBAX wavelength dispersive electron microprobe, with on-line data reduction (PAP correction routine). Standard operating conditions for the determination of major elements were 15 kV acceleration voltage and 20 nA beam current. In several of the samples (1/9.60, 4/64.50, H 8, some points on H 1) fluorine was analysed

with 5 kV acceleration voltage, to avoid excessive absorption. However, this procedure was more time-consuming, and gave no systematic differences in average concentrations or analytical error from analyses at 15 kV; the use of this method was therefore discontinued.

Several natural and synthetic mineral standards were used for major element calibration, F was standardized with fluorapatite from Cerro de Mercado, Durango, Mexico having 3.54 wt.% F (Young *et al.*, 1969). The analytical precision of fluorine is worse than most other major elements determined by electron microprobe. Repeated analyses of the Durango apatite standard and a 'pooled estimate of variance' of the complete set of apatite and biotite analyses from Fen, yield a  $1\sigma$  standard deviation of 9% relative.

The trace components La, Ce, Nd, Sr and S in apatite were determined in a separate set of microprobe analyses, using 15 kV (in some cases 20 kV) acceleration voltage and 50 to 80 nA beam current, with a 10  $\mu\text{m}$  defocused electron beam. Each REE single analysis represents a set of 10 closely spaced individual microprobe analyses around the points analysed for major elements. Synthetic oxide glasses produced by R. Åmli (Åmli and Griffin, 1975) and the REE silicate glasses of Drake and Weill (1972) were used as primary REE standards. We obtained the following results from repeated analysis of the Durango apatite ( $\pm 1\sigma$  standard error;  $\text{RE}_2\text{O}_3$  concentrations from Rønso (1989) are given in parentheses):  $\text{La}_2\text{O}_3$ :  $0.395 \pm 0.040$  (0.474),  $\text{Ce}_2\text{O}_3$ :  $0.466 \pm 0.043$  (0.563) and  $\text{Nd}_2\text{O}_3$ :  $0.143 \pm 0.032$  (0.148).

### Results

In Tables 1 and 2, each column represents an average of several point analyses on a single homogeneous grain or on several homogeneous grains with indistinguishable fluorine content. Assuming a fixed number of OH + Cl + F (i.e. disregarding the possibility of  $\text{O}^{2-}$  for OH<sup>-</sup> substitution),  $X_{\text{OH}} = 1 - X_{\text{F}} - X_{\text{Cl}}$ , where  $X_{\text{F}}$  and  $X_{\text{Cl}}$  are derived directly from the analyses. Both  $X_{\text{F}}$  and the  $X_{\text{F}}/X_{\text{OH}}$  ratio used in some of the subsequent calculations in this paper are critically dependent upon the procedure used for calculation of structural formulae from the microprobe analyses. This is no trivial problem for apatites and phlogopites. The justification for the fixed numbers of cations used is discussed below.

For thermometrical and barometrical applications, only minerals coexisting in equilibrium at the time of crystallization should be combined. In rocks with uniform apatite and phlogopite com-

Table 1

Major element composition of apatites

Ref. no.	1/9.60	1/21.70	1/21.70	1/21.70	4/64.50	C 27	H 1-2	H 1-2	H 1-2	H 1	H 1	H 8	3/84.80
	13 Cumulate	5 Carbonatite	3	5	17 Carb.	9 Carb.	5 Carb. vein	3	2	9 Phlogopite rock	3	4 Carb.	6 Carb.
	1	2	3	4	5	6	7	8a	8b	9a	9b	10	11
		Phenox.	Incl.	Phenox.									
Weight percent oxides													
CaO	54.30	56.11	55.56	55.93	55.37	55.90	55.17	55.28	54.73	53.51	53.31	54.68	54.69
Na <sub>2</sub> O	0.29	0.33	0.32	0.30	0.24	0.14	0.15	0.14	0.21	0.19	0.20	0.21	0.29
La <sub>2</sub> O <sub>3</sub>	0.11	0.14	0.15	0.13	0.10	0.10	0.16	0.10	0.10	0.18	0.16	0.10	0.15
Ce <sub>2</sub> O <sub>3</sub>	0.26	0.30	0.30	0.29	0.22	0.26	0.33	0.23	0.21	0.35	0.34	0.22	0.34
Nd <sub>2</sub> O <sub>3</sub>	0.16	0.14	0.18	0.13	0.15	0.17	0.15	0.10	0.14	0.17	0.13	0.15	0.23
P <sub>2</sub> O <sub>5</sub>	40.98	41.94	41.59	41.54	41.80	41.68	42.17	41.27	41.35	42.65	42.78	41.96	39.94
SiO <sub>2</sub>	0.09	0.32	0.54	0.43	0.03	0.05	0.28	0.23	0.06	0.02	0.03	0.14	0.50
F	2.77	1.24	1.40	1.56	2.49	3.21	2.47	2.88	2.03	3.07	2.44	2.52	1.20
Cl	0.02	0.02	0.04	0.03	0.03	0.01	0.02	0.01	0.02	0.01	0.02	0.02	0.07
F=O	-1.16	-0.52	-0.59	-0.66	-1.05	-1.35	-1.04	-1.21	-0.85	-1.29	-1.03	-1.06	-0.50
Cl=O	-0.01	-0.01	-0.01	-0.01	-0.01	-0.00	-0.00	-0.00	-0.01	-0.00	-0.01	-0.01	-0.02
Sum	97.82	100.01	99.48	99.67	99.37	100.16	99.86	99.03	98.00	98.85	98.39	98.94	96.89
Structural formulae based on Ca+Na+La+Ce+Nd = 10.000 and F+Cl+OH = 2.000													
Ca	9.875	9.865	9.867	9.874	9.894	9.923	9.923	9.926	9.903	9.904	9.900	9.902	9.861
Na	0.095	0.105	0.103	0.096	0.078	0.045	0.049	0.045	0.069	0.064	0.067	0.069	0.095
La	0.008	0.007	0.007	0.007	0.006	0.006	0.007	0.007	0.007	0.009	0.009	0.006	0.009
Ce	0.018	0.013	0.013	0.013	0.013	0.016	0.013	0.013	0.013	0.016	0.016	0.014	0.021
Nd	0.003	0.011	0.011	0.011	0.009	0.010	0.008	0.008	0.008	0.008	0.008	0.009	0.014
P	5.889	5.827	5.836	5.795	5.902	5.846	5.993	5.856	5.912	6.238	6.278	6.004	5.691
Si	0.015	0.053	0.090	0.071	0.005	0.008	0.047	0.039	0.010	0.003	0.005	0.024	0.084
F	1.485	0.650	0.738	0.821	1.321	1.700	1.311	1.540	1.090	1.657	1.319	1.347	0.648
Cl	0.007	0.007	0.011	0.009	0.009	0.002	0.005	0.002	0.007	0.002	0.007	0.007	0.021
OH	0.508	1.343	1.251	1.169	0.670	0.298	0.684	0.457	0.903	0.341	0.674	0.646	1.331
SumCAT:	15.90	15.88	15.93	15.87	15.91	15.85	16.04	15.89	15.92	16.24	16.28	16.03	15.77
SumCH:	49.44	49.27	49.47	49.19	49.48	49.25	50.13	49.42	49.56	51.17	51.37	50.08	48.74
X <sub>F</sub>	0.742	0.325	0.369	0.411	0.661	0.850	0.656	0.770	0.545	0.828	0.660	0.673	0.324
X <sub>Cl</sub>	0.004	0.003	0.006	0.005	0.005	0.001	0.002	0.001	0.004	0.001	0.004	0.004	0.010
X <sub>OH</sub>	0.254	0.672	0.625	0.585	0.335	0.149	0.342	0.229	0.452	0.170	0.337	0.323	0.666

n: Number of single analyses in each mean. SumCAT: Total number of cations. SumCH: Total cationic charge.

positions, we assume that the minerals have equilibrated throughout the sample volume, either during primary crystallization from the melt, or at some stage of the subsequent cooling history. Where there are variations in the composition of either one or both of the minerals, we have been careful to combine only mineral pairs in direct grain contact. Pairs of apatite and phlogopite assumed to coexist in equilibrium are identified by identical reference numbers in Tables 1 and 2. In cases where only one of the minerals in a sample or in a domain within a sample shows compositional variations, and the other stays homogeneous, the variations are indicated by the use of indexes *a* and *b* in the tables; these analyses should be combined with the corresponding analysis of their homogeneous partner.

**Apatite.** The apatite analyses show variable fluorine (1.27–3.29 wt.%), but uniformly low sodium and silica contents (Table 1). The analysed REE sum to  $\leq 0.72$  weight per cent oxides, given the steep, LREE-enriched distribution patterns of these rocks (Andersen, 1987), heavier

REE are considered to be insignificant for the total. S and Sr fall below the detection limits, assumed to be of the order of 0.01 wt.% and 0.1 wt.%, respectively. Chlorine concentrations are uniformly low, less than 0.03 wt.% in most analyses (detection limit: ca 0.01 wt.%). Several samples (1/9.60, 4/64.50, C 27, H 8, 3/84.80) have uniform apatite compositions, where neither zoning nor between-grain differences in F contents can be detected. In 1/21.70 and H 1–2 there is considerable variation in composition between grains, no zoning has, however, been detected. It should be noted that the range of apatite composition in phlogopite-rich metasomatic rims lining sylvite veins (H 1) largely overlaps with macrocrysts embedded in the veins (H 1–2).

Substitution mechanisms in apatites from carbonatites have recently been reviewed by Hogarth (1989). Starting with a simplified formula of the type  $\text{Ca}_{10}(\text{PO}_4)_6(\text{F}, \text{Cl}, \text{OH})_2$ , the apatite analyses have been recalculated to structural formulae assuming  $\text{Ca} + \text{Na} + \text{La} + \text{Ce} + \text{Nd} = 10.000$  cations (Le Bas and Handley, 1979). This gives P + Si in the range 5.71–6.28, so,

Table 2

Major element composition of phlogopites

	1/9.60	1/21.70	1/21.70	1/21.70	4/64.50	C 27	H 1-2	H 1-2	H 1	H 8	H 8
	Cumulate	Carbonatite			Carb.	Carb.	Carb. vein		Ph. rock	Carb.	
n	6	4	2	2	3	11	8	6	8	2	6
Ref. no.	1	2	3	4	5	6	7	8	9	10a	10b
		core <sup>1</sup>	rim <sup>2</sup>	core <sup>1</sup>							
Weight percent oxides											
SiO <sub>2</sub>	39.55	39.09	40.88	40.22	41.51	41.27	40.71	40.47	42.15	41.39	41.90
TiO <sub>2</sub>	0.32	0.34	0.40	0.36	0.14	0.16	1.28	0.63	1.04	0.09	0.10
Al <sub>2</sub> O <sub>3</sub>	11.73	12.86	8.32	10.41	10.71	11.48	11.25	11.10	11.47	12.16	11.32
FeO	5.75	5.51	8.33	6.87	6.12	5.73	7.51	7.53	6.24	4.21	4.23
MnO	0.11	0.09	0.10	0.09	0.08	0.10	0.15	0.21	0.08	0.08	0.08
MgO	23.11	24.60	23.85	24.26	25.52	26.96	23.48	23.08	23.98	26.70	26.32
CaO	0.00	0.03	0.11	0.08	0.00	0.07	0.10	0.12	0.00	0.00	0.00
Na <sub>2</sub> O	0.42	0.53	0.40	0.46	0.04	0.37	0.09	0.21	0.08	0.47	0.38
K <sub>2</sub> O	9.40	9.55	9.43	9.46	9.52	9.29	9.69	9.68	9.71	9.70	9.83
F	2.17	0.31	0.23	0.30	1.20	1.83	0.95	0.99	1.67	1.65	1.85
Cl	0.03	0.00	0.00	0.00	0.02	0.00	0.02	0.02	0.02	0.01	0.02
F=O	-0.92	-0.13	-0.09	-0.13	-0.50	-0.77	-0.40	-0.41	-0.71	-0.69	-0.78
Cl=O	-0.01	0.00	0.00	0.00	-0.00	0.00	-0.00	-0.01	-0.00	-0.00	-0.00
Sum	94.61	96.73	95.85	96.30	97.95	99.90	98.49	97.21	98.58	99.22	98.56
Structural formulae based on Si+Al+Ti+Mg+Fe+Mn = 14.000 and F+Cl+OH = 4.000											
Si	5.956	5.709	6.115	5.943	5.963	5.779	5.916	5.970	6.054	5.843	5.976
Al	2.082	2.214	1.467	1.813	1.813	1.895	1.927	1.930	1.942	2.023	1.903
Ti	0.036	0.037	0.045	0.040	0.015	0.017	0.140	0.070	0.112	0.010	0.011
Fe <sub>2+</sub>	0.724	0.673	1.042	0.849	0.735	0.671	0.913	0.929	0.749	0.497	0.505
Mn	0.014	0.011	0.013	0.011	0.010	0.012	0.018	0.026	0.010	0.010	0.010
Mg	5.188	5.356	5.318	5.344	5.464	5.627	5.086	5.075	5.133	5.618	5.596
Ca	0.000	0.005	0.018	0.013	0.000	0.011	0.016	0.019	0.000	0.000	0.000
Na	0.123	0.150	0.116	0.132	0.011	0.100	0.025	0.060	0.022	0.129	0.105
K	1.806	1.779	1.800	1.783	1.744	1.659	1.796	1.822	1.779	1.747	1.789
F	1.036	0.143	0.107	0.141	0.543	0.810	0.437	0.460	0.761	0.735	0.835
Cl	0.008	0.000	0.000	0.000	0.004	0.000	0.004	0.006	0.004	0.002	0.004
OH	2.956	3.857	3.893	3.859	3.453	3.190	3.559	3.534	3.235	3.263	3.161
SumCAT:	15.93	15.93	15.93	15.93	15.76	15.77	15.84	15.90	15.80	15.88	15.89
SumCH:	44.00	43.65	43.74	43.72	43.52	43.27	43.89	43.93	44.07	43.60	43.77
X <sub>F</sub>	0.259	0.036	0.027	0.035	0.136	0.203	0.109	0.115	0.190	0.184	0.209
X <sub>Cl</sub>	0.002	0.000	0.000	0.000	0.001	0.000	0.001	0.002	0.001	0.000	0.001
X <sub>OH</sub>	0.739	0.964	0.973	0.965	0.863	0.797	0.890	0.884	0.809	0.816	0.790
X <sub>ph</sub>	0.865	0.893	0.886	0.891	0.911	0.938	0.848	0.846	0.871	0.936	0.933
X <sub>Ann</sub>	0.089	0.099	0.104	0.101	0.118	0.106	0.126	0.138	0.125	0.081	0.082
X <sub>Sid</sub>	0.038	0.000	0.000	0.000	0.000	0.000	0.000	0.000	0.000	0.000	0.000
FIV	1.817	2.832	2.956	2.834	2.239	2.068	2.255	2.232	2.007	2.107	2.033

n: Number of single analyses in each mean. SumCAT: Total number of cations. SumCH: Total cationic charge.

FIV =  $1.52 X_{ph} + 0.42 X_{Ann} + 0.2 X_{Sid} - \log(X_F/X_{OH})$ , i.e. the "Fluorine intercept value" of Munoz (1984).

1: Normally pleochroic core of zoned phlogopite. 2: Inversely pleochroic rim against apatite inclusion.

although substitution of carbon in the form of CO<sub>3</sub>, CO<sub>3</sub>OH or CO<sub>3</sub>F groups replacing PO<sub>4</sub> tetrahedra is possible in apatite (McConnell, 1973; Le Bas and Handley, 1979; Sommerauer and Katz-Lehnert, 1985b; Binder and Troll, 1989), it must be very small or negligible here. The CO<sub>3</sub>F substitution will not therefore have any significant effect on the total fluorine content.

The apatites range from fluorapatite ( $X_F > 0.5$ , maximum  $X_F = 0.8$ ) to hydroxyapatite ( $X_F = 0.34-0.44$ ). The low fluorine content is restricted to two samples, the apatite-rich carbonatite 1/21.70 and the baddeleyite-bearing sample 3/84.80.

*Phlogopite.* The present phlogopite analyses (Table 2) fall within the high-MgO region of the range of volatile-free phlogopite analyses reported from phlogopite-amphibole *søvite*, apatite rocks and contact metasomatic phlogopite rocks by Andersen (1989), with MgO > 23 wt.%. Because the present study is concerned mainly with the F/OH ratio of the phlogopite, point analyses with minor differences in Mg/(Mg + Fe) have been averaged (for a more detailed discussion of mica composition in these rocks, see Andersen, 1989).

K<sub>2</sub>O is low in the phlogopite, less than 10 wt.%. Low-potassium (alkali deficient) phlo-

gopites were reported from the Sarfartoq carbonatite complex, Greenland (Secher and Larsen, 1980) and from fenites in the Loe Shilman carbonatite complex, Pakistan (Mian and LeBas, 1987). In the Fen complex, low K in mica has been related to leaching of alkalis during initial post-magmatic re-equilibration or metasomatism (Andersen, 1984, 1989). Using a simplified structural formula  $K_2Mg_6Al_2Si_6O_{20}(OH, F)_4$  and keeping the possibility of alkali deficiency in mind, structural formulae have been based on  $Si + Al + Ti + Mg + Fe + Mn = 14.000$ , rather than on a fixed number of oxygens or total cations. OH has been calculated by difference, assuming  $F + Cl + OH = 4.000$ . Recalculated in this way,  $Na + Ca + K$  sum to 1.77 to 1.90 cations, suggesting that postmagmatic leaching processes have only had limited effects in these rocks. All but one of the present samples have  $Si + Al < 8.000$  cations, suggesting substitution of minor amounts of titanium and ferric iron in the tetrahedral positions (e.g. Faye and Hogarth, 1969). This is especially pronounced in the inversely pleochroic rims of zoned crystals in 1/21.70, which also have the highest FeO content of all the phlogopites analysed (ref. no. 3 in Table 2).

Hydroxyl-ion is the dominant anion in the phlogopites,  $X_{OH} \geq 0.74$ . Chlorine in the phlogopites is close to the detection limit ( $< 0.03$  wt. %). There is a sympathetic variation of F in apatite and phlogopite, in samples containing fluorapatite, fluorine in phlogopite ranges from 0.44 to 2.17 wt. %. Recalculated, this corresponds to a range of  $X_F$  from ca. 0.11 to 0.26 (which is significantly less than in the coexisting apatite). In sample 1/21.70, hydroxyapatite coexists with phlogopite with less than 0.15 wt. % F ( $X_F \approx 0.03$ ). The pattern of variation within samples resembles that of the apatite, with uniform compositions in 1/9.60, 4/64.50 and C 27, while H 1-2 and H 8 show minor differences in  $X_F$  between different homogeneous grains. In H 1-2, this variation is relatively less in phlogopite ( $X_F = 0.109$  to 0.115) than in apatite ( $X_F = 0.545$  to 0.770). In 1/21.70 the inversely pleochroic rims of the zoned biotite have lower  $X_F$  than the normally pleochroic cores of the crystals (compare columns 3 and 4 in Table 2). The phlogopite in the contact metasomatic rock (H 1) is homogeneous, with  $X_F$  similar to that of phlogopite from søvite.

### The distribution of fluorine between apatite and phlogopite

#### Geothermometry

The F-OH exchange between mica and apatite depends upon temperature and the composition

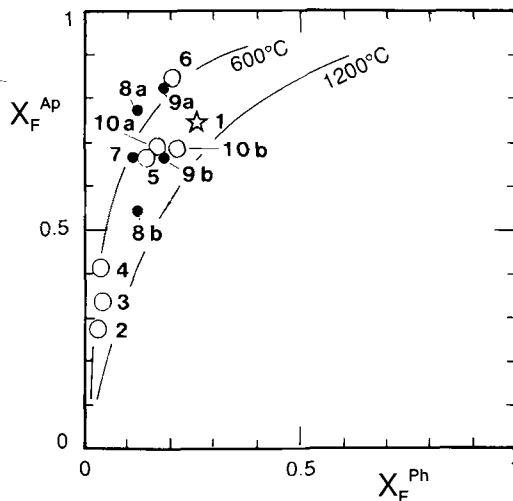


FIG. 2. Distribution of fluorine between coexisting apatite and phlogopite. Data from Tables 1 and 2. Symbols: Star = apatite cumulate. Open circle = carbonatite. Filled circles: Søvite-veined, contact metasomatized country rock. Isotherms for apatite-phlogopite ( $X_{Ann} = X_{Sid} = 0$ ) in equilibrium according to Ludington (1978). Apatite-phlogopite pairs are identified by reference numbers (ref. nos in Tables 1, 2 and 3).

of the mica, high  $Mg/(Mg + Fe)$  and low octahedral Al favouring  $F^-$  in the anion sites of the mica (Ludington, 1978). The F-OH distribution between coexisting apatite and biotite was suggested as a geothermometer by Stormer and Carmichael (1971). Ludington's (1978) calibration of this thermometer accounts for the effect of mica composition on the partition coefficient for F between biotite and apatite, and is expressed by the formula

$$T = 1100 / (\log(X_F/X_{OH})_{Ap} - \log((X_F/X_{OH})_{Bi} - [1.107X_{Ann} + 1.444X_{Sid}])) \quad (1)$$

where  $X_F$  and  $X_{OH}$  are mole fractions of fluoride and hydroxyl ions in the anion positions of apatite and biotite. The terms in square brackets refer to the cation distribution of the mica:  $X_{Ann} = Fe^{VI} - 5Al^{VI}/\Sigma_{Oct}$ ,  $X_{Sid} = 6Al^{VI}/\Sigma_{Oct}$ .

The distribution of fluorine between coexisting apatite and phlogopite in the carbonatites from Fen is illustrated in Fig. 2, with isotherms for apatite-phlogopite pairs at 600 °C and 1200 °C. Temperatures estimated from equation (1) are listed in Table 3. The uncertainty in the temperatures caused by analytical error in fluorine is considerable; the  $\pm 1\sigma$  standard error in  $X_F$  propagates to a temperature uncertainty of  $\pm 50$ -

Table 3 Geothermometry and HF-barometry

Sample	Ref. no.	T °C	$\sigma$	$\log(f_{\text{HF}}/f_{\text{H}_2\text{O}})$	
1/9.60	1	1160	+49, -45	-3.29	+0.10
1/21.70	2	821	+14	-4.76	+0.05
	3	630	+14, -13	-5.30	$\pm 0.07$
	4	666	+14, -13	-5.08	$\pm 0.06$
4/65.50	5	864	+22	-4.04	$\pm 0.07$
C24	6	618	+20, -19	-4.36	$\pm 0.10$
H1-2	7	770	+26, -25	-4.31	$\pm 0.10$
	8a	600	+27, -26	-4.66	$\pm 0.15$
	8b	1077	+55, -54	-3.81	$\pm 0.13$
H1	9a	661	+23, -21	-4.26	$\pm 0.10$
	9b	1133	+66, -61	-3.51	$\pm 0.13$
H8	10a	982	+58, -54	-3.75	$\pm 0.14$
	10b	1092	+58, -54	-3.55	$\pm 0.12$
3/84.80	11	700*		-5.12	$\pm 0.01$

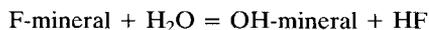
Temperatures are calculated using the biotite-apatite OH-F exchange thermometer of Ludington (1978). Relative HF-fugacities have been estimated using equations (2) and (4) in the text. \*: Model temperature in phlogopite-free sample. Errors in temperature and relative HF Fugacity are based on  $\pm 1\sigma$  standard error in fluorine analyses.

60 °C at  $T > 1100$  °C, but to less than  $\pm 25$  °C in the 600–650 °C range.

The biotite-apatite geothermometer yields temperature estimates in the range 1160 to 618 °C for the calcite carbonatites and apatite-rich cumulates (Table 3). Consistent overestimation of  $X_{\text{F}}$  in apatite due to the neglect of a  $\text{CO}_3\text{F}$  substitution effect would cause underestimation of temperature. The magnitude of this effect cannot be evaluated from the present data, but as was argued above, it is unlikely to exceed the effect of analytical uncertainty.

#### Hydrogen fluoride fugacity

When volatile-bearing minerals such as biotite and apatite interact with a fluid phase and/or volatile-containing magma, OH-F exchange reactions of the type



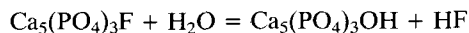
can buffer the hydrogen fluoride fugacity of the system. Such reactions are also important as potential 'HF-barometers', which can be used to monitor the evolution of the HF fugacity of a magmatic system during cooling, whether or not they have acted as buffer equilibria.

From experimental data combined with thermodynamical analysis of coupled F-OH and Fe-Mg exchange in micas, Munoz and Ludington (1974) and Munoz (1984) have derived a relationship between biotite composition, the relative hydrogen fluoride fugacity ( $\log f_{\text{HF}}/f_{\text{H}_2\text{O}}$ ) and absolute temperature,

$$\log f_{\text{HF}}/f_{\text{H}_2\text{O}} = -2100/T - [1.523 X_{\text{Ph}} + 0.416 X_{\text{Ann}} + 0.200 X_{\text{Sid}}] + \log(X_{\text{F}}/X_{\text{OH}})_{\text{Bi}} \quad (2)$$

where  $f_{\text{HF}}$  and  $f_{\text{H}_2\text{O}}$  are hydrogen fluoride and water fugacities, respectively,  $X_{\text{Ph}} = \text{Mg}^{\text{VI}}/\Sigma\text{oct}$ ,  $X_{\text{Ann}} = \text{Fe}^{\text{VI}} - 5\text{Al}^{\text{VI}}/\Sigma\text{oct}$ ,  $X_{\text{Sid}} = 6\text{A}^{\text{VI}}/\Sigma\text{oct}$  and  $X_{\text{F}}$  and  $X_{\text{OH}}$  are fluoride and hydroxyl mole fractions in the anion sites of the mica.

Assuming ideal OH-F mixing in apatite (Tacker and Stormer, 1989), the equilibrium constant for the apatite-fluid exchange reaction



is given by

$$\log K_{\text{Ap}} = \log(f_{\text{HF}}/f_{\text{H}_2\text{O}}) - \log(X_{\text{F}}/X_{\text{OH}})_{\text{Ap}}$$

Korshinskij (1981) established an empirical expression for this equilibrium constant, which is linear in temperature:

$$\log(f_{\text{HF}}/f_{\text{H}_2\text{O}}) = 0.0085 T - 13.25 + \log(X_{\text{F}}/X_{\text{OH}})_{\text{Ap}}$$

this has been used as a HF barometer by Yardley (1985) and Hogarth *et al.* (1987). Unfortunately, a relative hydrogen fluoride fugacity calculated from this equation will generally differ from that obtained from a coexisting biotite at the equilibrium temperature indicated by the apatite-biotite thermometer.

If equilibrium between biotite and apatite has been obtained, Ludington's (1978) calibration of the apatite-biotite geothermometer [equation (1)] describes the relationship between temperature and mineral compositions. By combining equations (1) and (2), and allowing  $X_{\text{Ann}} + X_{\text{Ph}} + X_{\text{Sid}} = 1.0$ , an expression relating  $\log(f_{\text{HF}}/f_{\text{H}_2\text{O}})$  to the composition of apatite coexisting with biotite is obtained:

$$\log(f_{\text{HF}}/f_{\text{H}_2\text{O}}) = \log(X_{\text{F}}/X_{\text{OH}})_{\text{Ap}} - 1.523 - 0.121 X_{\text{Sid}} - 3200/T \quad (3)$$

Because the present phlogopites contain negligible octahedral aluminium, the relative HF fugacity is independent of biotite composition, and equation (3) is reduced to:

$$\log(f_{\text{HF}}/f_{\text{H}_2\text{O}}) = \log(X_{\text{F}}/X_{\text{OH}})_{\text{Ap}} - 1.523 - 3200/T \quad (4)$$

This equation necessarily gives  $\log(f_{\text{HF}}/f_{\text{H}_2\text{O}})$  values consistent with those calculated from coexisting phlogopite at the equilibrium temperature, and is used in the present study to describe the relationship between apatite composition, relative hydrogen fluoride fugacity and temperature.

Estimates of relative hydrogen fluoride fugacity at the apatite-phlogopite equilibrium temperature, calculated from equations (2) and (4) are

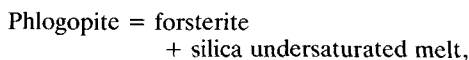
given in Table 3, and are plotted against inverse temperature in Fig. 3. The uncertainty of the estimates is related to the uncertainty in temperature, and amounts to less than  $\pm 0.15$  log units. Sample 3/84.80 does not contain phlogopite, and  $\log(f_{\text{HF}}/f_{\text{H}_2\text{O}})$  is given for a reference temperature of 700°C. The majority of samples yield  $\log(f_{\text{HF}}/f_{\text{H}_2\text{O}})$  values between  $-4.8$  and  $-3.3$ . Two samples (1/21.70 and 3/84.80) stand out from the rest, with  $\log(f_{\text{HF}}/f_{\text{H}_2\text{O}})$  below  $-5.0$ , but at temperatures within the range of the 'high' HF-fugacity samples. Fig. 3 shows a good negative correlation with inverse temperature within the 'high' and 'low' HF-fugacity groups.

### Discussion

#### *Crystallization history of calcite carbonatite magma*

Apatite and phlogopite have formed throughout the crystallization history of calcite carbonatite in the Fen complex, from the early evolution of carbonatite magma in middle crust, to intrusion and *in situ* crystallization at shallow depth. Experimental studies of simplified calcite carbonatite melt systems have shown that apatite will precipitate as the first liquidus phase, or coprecipitate with calcite over wide composition and temperature ranges (Wyllie, 1966; Biggar, 1969).

The maximum thermal stability of phlogopite is given by the incongruent melting reaction



which is located close to 1200°C over a wide pressure range (Yoder and Kushiro, 1969). This reaction sets an absolute upper temperature limit for the crystallization of phlogopite phenocrysts from silica undersaturated magmas. In their study of mafic silicate intrusions related to the Fen complex, Griffin and Taylor (1975) presented mineralogical data from phlogopite porphyritic lamprophyre dykes (damtjernite) to suggest that their phenocryst assemblage (phlogopite + nepheline + apatite + pyroxene) crystallized at temperatures below 1200°C, and that the matrix of the dykes solidified between 1100 and 900°C. Those intrusions, as well as similar rocks studied by Dahlgren (1984, 1987), show well-developed two-liquid structures, suggesting that a calcite-carbonatite magma has exsolved from the mafic silicate magma during its crystallization. When a magma unmixes into silicate and carbonatite liquids, both immiscible fractions must be in simultaneous equilibrium with the phenocryst

assemblage of the precursor, in this case with a mineral assemblage including apatite and phlogopite (e.g. Treiman and Essene, 1985). It therefore seems reasonable to assume that the calcite carbonatite magmas in the Fen complex have formed somewhere in the interval 1000 to 1200°C, and that they have been saturated in phlogopite and apatite from the start. In the presence of an aqueous fluid phase, calcite carbonatite magmas have solidus temperatures in the range 625–650°C (Wyllie, 1966).

The highest temperature estimate obtained from the apatite cumulate ( $1160 \pm 50^\circ\text{C}$ ) approaches the maximum liquidus temperature, and thus confirms the early magmatic nature of apatite cumulate (Andersen, 1986a). The carbonatite samples show a wide range of temperatures, ranging from 1092°C to temperatures near the solidus ( $618 \pm 20^\circ\text{C}$ ). This wide variation in temperature reflects continual precipitation and/or equilibration of the two minerals during most of the crystallization history of the carbonatite magma. The higher part of the temperature range (1092–821°C) may reflect crystallization of phenocrysts during early fractionation, ascent and emplacement of the magma, and is our best estimate of intrusive temperatures for the Fen calcite carbonatite magma. In sample H 8, the apatite + phlogopite equilibration seems to have terminated close to 1000°C, whereas it has continued to temperatures at, or close to, the solidus in the other carbonatite samples. Fluid inclusions in matrix minerals in these carbonatites suggest that the rocks interacted with fluids of magmatic descent at temperatures less than 300°C (Andersen, 1988b). Since none of the apatite-phlogopite pairs give such low temperatures, the fluorine distribution between these minerals cannot have been affected by the low-temperature re-equilibration processes. This suggests that the presence of a carbonatite liquid is essential for the exchange of F and OH between the two minerals. In this respect the apatite-phlogopite pair differs from both the iron-titanium oxides and coexisting calcite and dolomite, which are easily affected by re-equilibration in the carbonatite environment (Gittins, 1979; Andersen, 1983, 1984).

The søvite-veined country-rock sample (H 1, H 1–2) yields a large range of temperatures, reflecting the variation in mineral composition. The 770°C temperature estimate obtained from one pair of macrocrysts (ref. no. 7, Table 3) may be a plausible intrusive temperature, whereas the lower values (600–666°C) can be due to near-solidus equilibration. Given the geological setting of this sample, the two very high temperatures

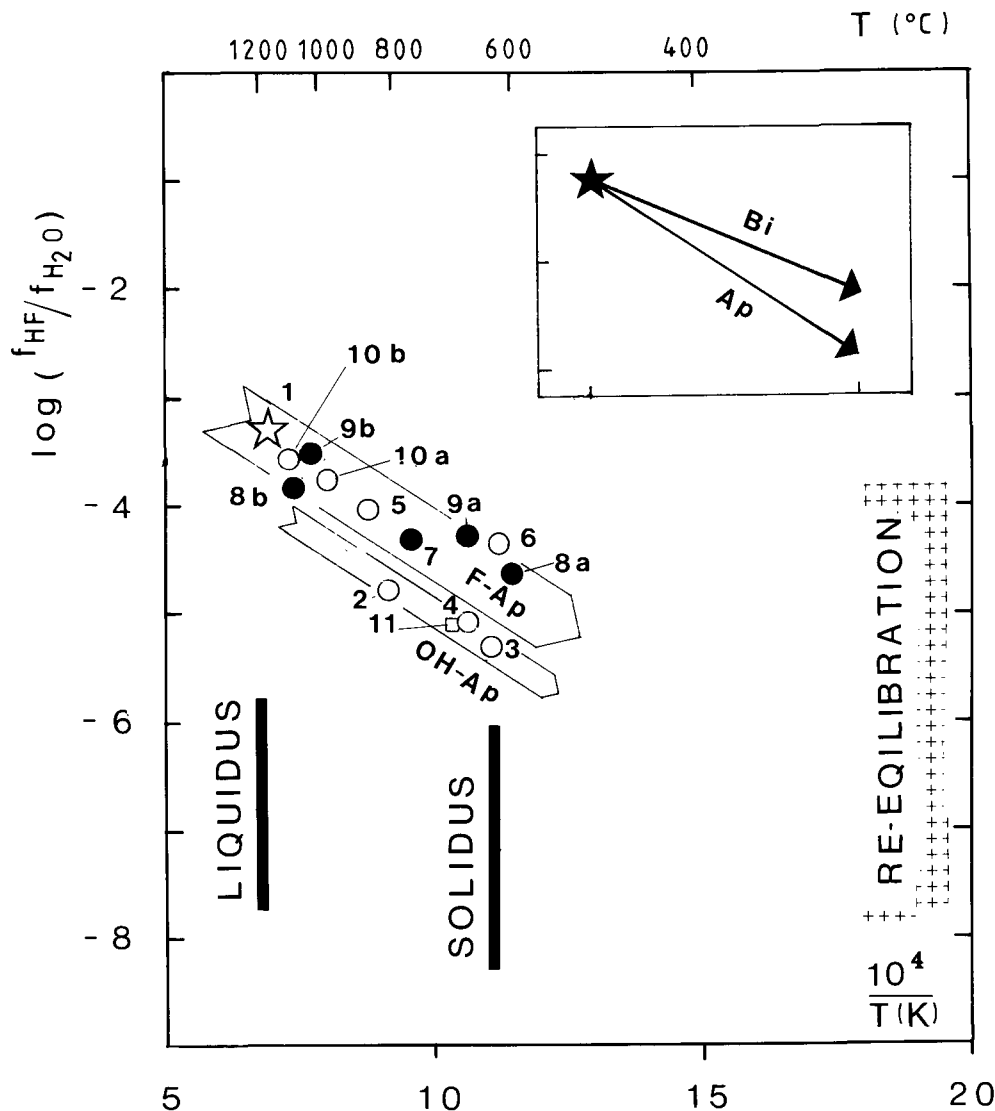


FIG. 3.  $\log(f_{\text{HF}}/f_{\text{H}_2\text{O}})$  vs.  $10^4/T$  diagram for the Fen apatites. The inset (same scale as main figure) shows possible cooling paths for apatite and biotite-buffered systems, having a common relative hydrogen fluoride fugacity at their starting temperature (filled star). The slopes of biotite (Bi) and apatite (Ap) buffered cooling paths are given by equations (2) and (4), respectively. Sample symbols in the main figure: Star = apatite cumulate. Open circle = carbonatite. Filled circles: Søvite-veined, contact metasomatized country rock. Square: carbonatite sample 3/84.80 at a reference temperature of 700 °C. Points are identified by reference numbers to apatite-phlogopite pairs (ref. nos in Tables 1, 2 and 3). The  $T < 1200$  °C estimate for the liquidus of the Fen 'Parent magma' has been derived from data on mafic silicate rocks in the complex by Griffin and Taylor (1975), the solidus (625–650 °C) is suggested by experimental data (Wyllie, 1966). The low-temperature re-equilibration field is derived from data by Andersen (1984, 1988b). The open arrows in the main figure are possible apatite-buffered cooling trends for the 'high' and 'low' HF-fugacity groups of samples discussed in the text. The trend at low  $\log(f_{\text{HF}}/f_{\text{H}_2\text{O}})$ -level is controlled by hydroxyapatite ( $X_{\text{F}} = 0.34\text{--}0.44$ ), the trend at high  $\log(f_{\text{HF}}/f_{\text{H}_2\text{O}})$  is controlled by fluorapatite with  $X_{\text{F}} = 0.5\text{--}0.8$ , corresponding to the compositional ranges observed in the present samples.

(1077 and 1133 °C) are hardly likely to represent apatite-phlogopite equilibria. It should be noted that these anomalous temperatures result from

combinations of comparatively fluorine-poor apatite ( $X_{\text{F}} = 0.55\text{--}0.66$ ) with ordinary phlogopite ( $X_{\text{F}} = 0.12\text{--}0.19$ ). From the shape of the iso-

therms in Fig. 2, it is obvious that selective secondary loss of fluorine from apatite would give erroneously high temperatures, if the phlogopite remained unaffected by the process. This is, however, unlikely to have occurred, since phlogopite is among the first minerals to break down during re-equilibration processes in the Fen carbonatites (Andersen, 1984). We therefore interpret these values as the results of erroneous combination of apatite and phlogopite compositions which have not been in equilibrium. Local disequilibrium is most likely to have occurred at the intrusive contact, where externally derived fluids may have influenced the composition of apatite crystallizing during emplacement of the veins. During subsequent cooling, the phlogopite composition has been equilibrated, at least on a millimetre scale, whereas some apatite crystals have been able to retain a memory of local, early crystallization conditions.

#### *Buffering of the HF-fugacity*

According to experimental findings (e.g. Wyllie, 1966) and fluid inclusion data (e.g. Andersen, 1986a), the fluid phase coexisting with crystallizing carbonatite magma is dominated by water, with alkali chlorides as the most abundant dissolved species. Assuming that the molar fraction of water in the fluid phase has remained high and constant throughout the crystallization history of the carbonatite magma, equilibrium between apatite or phlogopite with constant  $F/(F + OH)$  and the fluid phase may constrain the  $\log(f_{HF}/f_{H_2O})$  to a univariant curve controlled by the mineral composition during cooling, i.e. internally buffer the relative HF fugacity of the fluid phase (e.g. Yardley, 1985). Biotite- and apatite-controlled trends are straight lines when  $\log(f_{HF}/f_{H_2O})$  is plotted against inverse absolute temperature, and are given by isopleths defined by equations (2) and (4) respectively. It follows from these equations that a cooling-trend with apatite as the controlling phase is steeper than one controlled by biotite. The evolution of apatite- and biotite-buffered trends from a common starting-point is illustrated in the inset to Fig. 3. Which of the minerals will act as the controlling phase in a given system depends on their relative abundance.

The correlation between  $\log(f_{HF}/f_{H_2O})$  and  $1/T$  within the 'high' and 'low' HF-fugacity groups distinguished in Fig. 3 corresponds to what one would expect from systems where the hydrogen fluoride fugacity has been internally buffered during crystallization. The steep overall slopes of the two trends correspond to systems where

apatite, rather than biotite, acts as the controlling mineral. We have, accordingly, indicated two different trends in the figure, one buffered by fluorapatite, representing the 'high' HF-fugacity group, and one buffered by hydroxyapatite, representing the 'low' HF-fugacity samples (1/21.70 and 3/84.80). This representation is clearly an oversimplification, as there is considerable vertical spread along the fluorapatite trend, suggesting that more than one trend may be represented, or that biotite may also have had some control on the evolution of the HF fugacity of these carbonatites.

On the other hand, it is not possible to move from any point on the fluorapatite-buffered cooling trend into the *low*  $\log(f_{HF}/f_{H_2O})$  field of the hydroxyapatite-bearing samples by cooling in a single closed system buffered by apatite or phlogopite. A shift in the opposite direction could in principle occur along a trend strongly controlled by phlogopite, but only at temperatures considerably higher than any of those observed (i.e. at  $T \gg 1160^\circ\text{C}$ ), which is unrealistic in relation to the maximum temperature limit of  $1200^\circ\text{C}$  deduced for the generation of Fen calcite carbonatite magmas.

The  $\log(f_{HF}/f_{H_2O})$  levels of the mid-crustal cognate xenoliths 1/9.60 and 4/64.50 cannot be distinguished from that of dyke samples H 8 and C 27 and from macrocrysts and phlogopite-rich reaction-zones in H 1 and H 1-2. This suggests that the elevated  $\log(f_{HF}/f_{H_2O})$  level may represent a 'main igneous trend' in the Fen complex, where the fluid composition has been buffered by fluorapatite and/or phlogopite from early fractionation in the middle crust, to *in situ* crystallization and wall-rock reaction. The low  $\log(f_{HF}/f_{H_2O})$  trend, on the other hand, is represented only by cognate xenoliths of mid-crustal origin. The differences in HF fugacity must reflect processes at an early stage of the evolution of the calcite carbonatite magma, in the middle crust. We therefore suggest that the two trends at different HF-fugacity levels are the results of internally buffered evolution of calcite carbonatite magmas in two independent systems, which were similar in major element characteristics, but different in terms of volatile fugacities. This requires that calcite carbonatite magmas in the Fen complex have formed and evolved in two or more non-communicating magma chambers.

It may be suggested that the fluid phase coexisting with 'low' HF-fugacity carbonatite magma has been diluted by the addition of water. If so, this must have taken place at an early stage of evolution, when the magmas were still stored in magma chambers in the middle crust, under a

lithostatic pressure regime (Andersen, 1986a). Any water introduced at this stage must have originated from a deep source, different from the near-surface, convecting groundwater which has influenced some of the carbonatites after their final emplacement in the shallow crust (Andersen, 1984).

It is interesting to note that the evidence of the low HF-fugacity trend has not been wiped out by subsequent processes, even though the apatite-rich rocks were apparently transported to the surface in a rising magma (Andersen, 1986a). Samples 1/9.60 and 1/21.70 come from the same drill-core, with 12 m distance between them. Within this moderate volume, F-exchange with the host magma has not been able to obliterate the evidence of different primary crystallization conditions. This is further evidence that the F-OH distribution between apatite and phlogopite established during primary crystallization is not easily disturbed by secondary processes.

Using a slightly different apatite-biotite geothermometer and HF-barometer, Chernysheva *et al.* (1976) reported a change in  $\log(f_{\text{HF}}/f_{\text{H}_2\text{O}})$  from  $-5.6$  at  $630^\circ\text{C}$  (in 'stage 1 carbonatites') to  $-5.7$  at  $500^\circ\text{C}$  (in 'stage 2 carbonatites') in several carbonatite complexes from Siberia and Canada. They interpreted this as evidence that the carbonatites remained closed to fluorine during much of their history. In the coordinates of Fig. 3, their reported shift corresponds to a very flat trend, crosscutting possible cooling trajectories for systems buffered by apatite-fluid or phlogopite-fluid equilibria. It is therefore unlikely that the temperature and hydrogen fluoride fugacity changes observed by Chernysheva *et al.* (1976) are due to buffered cooling in a closed system.

#### HCl fugacity

The chlorine contents of the Fen apatite and phlogopites are low, approaching the detection limit by electron microprobe. No detailed quantification of the HCl fugacity is therefore justified. The low Cl-concentrations are not, however, evidence of low relative HCl fugacity in the fluid phase, since phlogopite-fluid and apatite-fluid partition coefficients for chlorine are considerably lower than for fluorine (Korshinskij, 1981; Munoz, 1984). Limiting HCl-fugacities can be determined from the maximum  $X_{\text{Cl}}$  for apatite and phlogopite (Tables 1 and 2), using the equations of Korshinskij (1981) for the apatite-fluid equilibrium and Munoz (1984) for the phlogopite-fluid equilibrium. Assuming  $X_{\text{Cl,max}} = 0.002$  for phlogopite ( $X_{\text{ph}} = 0.9$ ) and  $0.006$  for

apatite, these calculations yield  $\log(f_{\text{HCl}}/f_{\text{H}_2\text{O}})$  values close to  $-1$  at  $1000\text{ K}$  ( $727^\circ\text{C}$ ) and in the range of  $-2$  to  $-3$  at  $700\text{ K}$  ( $427^\circ\text{C}$ ). This suggests that the HCl-fugacity is 2-3 orders of magnitude higher than the HF-fugacity in fluids coexisting with calcite carbonatite magma in the Fen complex.

#### HF fugacity and element mobility

It is well known that the rare earth elements can form stable fluoride complexes in carbonatite magmas and aqueous fluids (e.g. Möller *et al.*, 1980; Alderton *et al.*, 1980; Högfeldt, 1982), which can influence their behaviour in magmatic and hydrothermal processes. The present carbonatites are not particularly strongly enriched in REE, but some of the samples have elevated niobium contents (H. Qvale pers. comm). The apatite in samples 1/9.60 and 4/64.50 contains abundant pyrochlore inclusions, and yields high  $\log(f_{\text{HF}}/f_{\text{H}_2\text{O}})$ . In low-temperature aqueous solutions, the  $\text{NbF}_6^-$  complex is even more stable than some of the REE-fluoride complex ions (Högfeldt, 1982). The coincidence between high Nb and high  $f_{\text{HF}}$  could suggest that fluoride complexing in fluid or magma may influence the behaviour of Nb during crystallization of carbonatite magma.

#### Conclusions

Despite the considerable uncertainty of temperature estimates based on the distribution of OH and F between apatite and phlogopite, the results obtained from carbonatites and apatite rocks from the Fen complex show that this geothermometer can be used to distinguish between primary magmatic carbonatites and rocks affected by post-magmatic re-equilibration, and to work out a crude cooling history for calcite carbonatites. In the Fen calcite carbonatites, low-temperature alteration seems not to have affected the F/OH ratios of apatite and phlogopite. This suggests that OH-F exchange between apatite, phlogopite and fluid during secondary processes is unimportant compared to the postmagmatic effects on the carbonate and iron-titanium oxide minerals in carbonatites.

The fluorine-content of apatite and phlogopite can be used to identify cooling trends characterized by different  $\log(f_{\text{HF}}/f_{\text{H}_2\text{O}})$ -levels. The  $\log(f_{\text{HF}}/f_{\text{H}_2\text{O}})-T^{-1}$  diagram is well suited for this purpose. In the Fen complex, apatite-phlogopite combined thermometry-HF barometry suggests two cooling trends characterized by different HF fugacity level. One of these is characterized by

relatively high  $\log(f_{\text{HF}}/f_{\text{H}_2\text{O}})$  level, and comprises both mid-crustal apatite cumulates, carbonatite dykes and contact metasomatic rocks. The other trend is characterized by low  $\log(f_{\text{HF}}/f_{\text{H}_2\text{O}})$  level, and is represented only by some apatite-rich rocks formed during fractionation of carbonatite magma in the middle crust. These trends reflect buffering of the hydrogen fluoride fugacity by apatite of different composition during the evolution of calcite carbonatite magmas in non-communicating mid-crustal magma chambers, and during the subsequent emplacement and crystallization of the magmas.

Our findings strongly suggest that even carbonatites which are closely similar in major element composition, and which have been emplaced close to each other within a short time span, may be the products of independent or semi-independent lines of magmatic evolution, rather than the differentiates of a single 'primitive' carbonatite parent magma.

#### Acknowledgements

Financial support from Nansenfondet, H. Bjørnum's Legat and H. and H. Reusch's Legat is gratefully acknowledged. The use of drill-core samples was authorized by AS Prospektering and Cappelen-Ulefoss. H. Qvale, G. Raade, B. B. Jensen, E.-R. Neumann and M. J. Le Bas have provided valuable suggestions and critical comments on the manuscript.

#### References

- Alderton, D. H. M., Pearce, J. A., and Potts, P. J. (1980) Rare earth mobility during granite alteration: evidence from southwest England. *Earth Planet. Sci. Lett.* **49**, 149–65.
- Åmli, R. and Griffin, W. L. (1975) Microprobe analysis of REE minerals using empirical correction factors. *Am. Mineral.* **60**, 599–606.
- Andersen, T. (1983) Iron ores in the Fen central complex, Telemark (S. Norway): Petrography, chemical evolution and conditions of equilibrium. *Norsk Geol. Tidsskr.* **63**, 73–82.
- (1984) Secondary processes in carbonatites: petrology of 'rødberg' (hematite–calcite–dolomite carbonatite) in the Fen central complex, Telemark (South Norway). *Lithos*, **17**, 227–45.
- (1986a) Magmatic fluids in the Fen carbonatite complex, S.E. Norway: Evidence of mid-crustal fractionation from solid and fluid inclusions in apatite. *Contrib. Mineral. Petrol.* **93**, 491–503.
- (1986b) Compositional variation of some rare earth minerals from the Fen complex (Telemark, S.E. Norway): Implications for the mobility of the rare earths in a carbonatite system. *Mineral. Mag.* **50**, 503–9.
- (1987) Mantle and crustal components in a carbonatite complex, and the evolution of carbonatite magma: REE and isotopic evidence from the Fen complex, S.E. Norway. *Chem. Geol., Isotope Geosci. Sect.* **65**, 147–66.
- (1988a) Evolution of peralkaline calcite carbonatite magma in the Fen complex, S.E. Norway. *Lithos*, **22**, 99–112.
- (1988b) Origin and significance of fluid inclusions in matrix minerals from the Fen carbonatite complex, Norway. *Geol. Soc. India Mem.* **11**, 25–36.
- (1989) Carbonatite-related contact metasomatism in the Fen complex, Norway: Effects and petrogenetic implications. *Mineral. Mag.* **53**, 395–414.
- and Taylor, P. N. (1988) Lead isotope geochemistry of the Fen carbonatite complex, S.E. Norway: Age and petrogenetic implications. *Geochim. Cosmochim. Acta*, **52**, 209–15.
- and Qvale, H. (1986) Pyroclastic mechanisms for carbonatite intrusion: Evidence from intrusives in the Fen central complex, S.E. Norway. *J. Geol.* **94**, 762–9.
- Bailey, J. C. (1980) Formation of cryolite and other aluminofluorides: a petrologic review. *Bull. geol. Soc. Denmark*, **29**, 1–45.
- Barth, T. F. W. and Ramberg, I. B. (1966) The Fen circular complex. In *Carbonatites* (Tuttle, O. F. and Gittins, J., eds). Interscience, New York, pp. 225–57.
- Bergstøl, S. and Svinndal, S. (1960) The carbonatite and peralkaline rocks of the Fen area. *Nor. geol. unders.* **208**, 99–105.
- Biggar, G. M. (1969) Phase relationships in the join  $\text{Ca}(\text{OH})_2\text{-CaCO}_3\text{-Ca}_3(\text{PO}_4)_2\text{-H}_2\text{O}$  at 1000 bars. *Mineral. Mag.* **37**, 75–82.
- Binder, G. and Troll, G. (1989) Coupled anion substitution in natural carbon-bearing apatites. *Contrib. Mineral. Petrol.* **101**, 394–401.
- Brøgger, W. C. (1921) Die Eruptivgesteine des Kristianiagebietes, IV. Das Fengebiet in Telemark, Norwegen. *Vit. Selsk. Skr., I Mat. Nat. Klasse 1920*, **1**, Kristiania, 494 pp.
- Chernysheva, Ye. A., Petrov, L. L., and Chernyshev, L. V. (1976) Distribution of fluorine between coexisting phlogopite and apatite in carbonatites and the behaviour of fluorine in the carbonatite forming process. *Geochem. Internat.* **13**, 3, 14–22.
- Clark, A. M. (1984) Mineralogy of the Rare Earth Elements. In *Rare Earth Geochemistry. Developments in Geochemistry 2* (P. Henderson, ed.), pp. 33–62. Elsevier, Amsterdam.
- Dahlgren, S. (1984) Carbonatite-, sulphide-, and silicate magma immiscibility in the Langeto dyke, Fen complex (abstract). *Geolognytt*, **20**, 20.
- (1987) *The saellitic intrusions in the Fen carbonatite alkaline rock province, Telemark, southeastern Norway*. Unpubl. Cand. Scient. Thesis, University of Oslo. 298 pp.
- Dawson, J. B. and Fuge, R. (1980) Halogen content of some African primary carbonatites. *Lithos*, **13**, 139–43.
- Drake, M. J. and Weill, D. F. (1972) New rare earth element standards for electron microprobe analysis. *Chem. Geol.* **10**, 179–81.
- Faye, F. H. and Hogarth, D. D. (1969) On the origin of

- 'reverse pleochroism' of a phlogopite. *Can. Mineral.* **10**, 25–34.
- Gittins, J. (1979) Problems inherent in the application of calcite–dolomite geothermometry to carbonatites. *Contrib. Mineral. Petrol.* **69**, 1–4.
- Griffin, W. L. and Taylor P.N. (1975) The Fen damkjernite: Petrology of a 'central complex kimberlite'. *Phys. Chem. Earth*, **9**, 163–77.
- Heinrich, E. W. (1966) *The geology of carbonatites*. Rand McNally & Co., Chicago, 555 pp.
- Hogarth, D. D. (1989) Pyrochlore, apatite and amphibole: distinctive minerals in carbonatite. In *Carbonatites, Genesis and evolution* (Bell, K., ed.), Unwin Hyman, London, pp. 105–148.
- , Chao, G. Y., and Townsend, M. G. (1987) Potassium and fluorine-rich amphiboles from the Gatineau area, Quebec. *Can. Mineral.* **25**, 739–53.
- Högfeldt, E. (1982) *Stability constants of metal-ion complexes. Part A: Inorganic ligands*. IUPAC Chemical Data Series, No. 21. Pergamon Press, Oxford.
- Knudsen, C. and Rønsbo, J. (1989) Distribution, texture and mineral chemistry of apatite from Qaqarsuk carbonatite complex, central West Greenland. In C. Knudsen: *En petrografisk, geokemisk og strukturel undersøgelse af Qaqarsuk karbonatit komplekset, specielt med henblik på genesis av apatit mineraliseringer i karbonatit*. Licentiatforhandling, Grønlands Geologiske Undersøgelse, København. 26 pp.
- Korshinskij, M. A. (1981) Apatite solid solution as indicators of the fugacity of  $\text{HCl}^0$  and  $\text{HF}^0$  in hydrothermal fluids. *Geochem. Internat.* **18**, 3, 44–60.
- Kresten, P. and Morogan, V. (1986) Fenitization at the Fen complex, southern Norway. *Lithos*, **19**, 27–42.
- Le Bas, M. J. and Handley, C. D. (1979) Variation in apatite composition in ijolitic and carbonatitic igneous rocks. *Nature*, **279**, 54–56.
- Ludington, S. (1978) The biotite–apatite geothermometer revisited. *Am. Mineral.* **63**, 551–53.
- McConnell, D. (1973) *Apatite, its crystal chemistry, mineralogy, utilization and geologic and biologic occurrences*. Springer Verlag, Berlin etc. (Applied Mineralogy, Vol. 5).
- Mian, I. and LeBas, M. J. (1987) The biotite–phlogopite series in fenites from the Loe Shilman carbonatite complex, NW Pakistan. *Mineral. Mag.* **51**, 397–408.
- Möller, P., Morteani, G., and Schley, F. (1980) Discussion of REE distribution patterns of carbonatites and alkalic rocks. *Lithos*, **13**, 171–9.
- Munoz, J. L. (1984) F–OH and Cl–OH exchange in micas with applications to hydrothermal ore deposits. *Reviews in Mineralogy*, **13**, 469–93.
- and Ludington, S. (1974) Fluorine–hydroxyl exchange in biotite. *Am. J. Sci.*, **274**, 396–413.
- Rønsbo, J. G. (1989) Coupled substitutions involving REEs and Na and Si in apatites in alkaline rocks from the Ilímaussaq intrusion, South Greenland. *Am. Mineral.*, **74**, 896–901.
- Sæther, E. (1957) The alkaline rock province of the Fen Area in southern Norway. *Det Kg. Nor. Vitensk. Selsk. Skr.* 1957, **1**, Trondheim, 148 pp.
- Secher, K. and Larsen, L. M. (1980) Geology and mineralogy of the Sarfartôq carbonatite complex, southern West Greenland. *Lithos*, **13**, 199–212.
- Sommerauer, J. and Katz-Lehnert, K. (1985a) Trapped melt inclusions in silicate–carbonate–hydroxyapatite from comb-layer alvikites from the Kaiserstuhl carbonatite complex (S.W. Germany). *Contrib. Mineral. Petrol.* **91**, 354–9.
- (1985b) A new partial substitution mechanism of  $\text{CO}_3^{2-}/\text{CO}_3\text{OH}^{3-}$  and  $\text{SiO}_4^{4-}$  for the  $\text{PO}_4^{3-}$  group in hydroxyapatite from the Kaiserstuhl alkaline complex (S.W. Germany). *Ibid.*, **91**, 360–8.
- Stormer, J. C. and Carmichael, I. S. E. (1971) Fluorine–hydroxyl exchange in apatite and biotites: a potential igneous geothermometer. *Ibid.*, **31**, 121–31.
- Tacker, R. C. and Stormer, J. C. (1989) A thermodynamic model for apatite solid solutions, applicable to high-temperature geologic problems. *Am. Mineral.*, **74**, 877–88.
- Treiman, A. H. and Essene, E. J. (1985) The Oka carbonatite complex, Quebec: Geology and evidence for silicate–carbonatite liquid immiscibility. *Ibid.*, **70**, 1101–13.
- Verschure, R. H. and Maijer, C. (1984) Pluri-metasomatic resetting of Rb–Sr whole-rock systems around the Fen peralkaline–carbonatitic ring complex, Telemark, South Norway. *Terra Cognita*, **4**, 191–2.
- Wyllie, P. J. (1966) Experimental studies of carbonatite problems: The origin and differentiation of carbonatite magmas. In *Carbonatites* (Tuttle, O. F. and Gittins, J., eds.). Interscience, New York, pp. 311–52.
- Yardley, B. W. D. (1985) Apatite composition and the fugacities of HF and HCl in metamorphic fluids. *Mineral. Mag.* **49**, 77–9.
- Yoder, H. S. and Kushiro, I. (1969) Melting of a hydrous phase: phlogopite. *Am. J. Sci.* **267-A**, 558–82.
- Young, E. J., Myers, A. T., Munson, E. L., and Conklin, N. M. (1969) Mineralogy and geochemistry of fluorapatite from Cerro de Mercado, Durango, Mexico. *U.S. Geol. Surv. Prof. Paper*, **650D**, 84–93.

[Manuscript received 22 April 1990;  
revised 22 June 1990]